Scientia Iranica B (2016) 23(6), 2595–2605

Sharif University of Technology
Scientia Iranica
Transactions B: Mechanical Engineering
www.scientiairanica.com

Comparison of ISPH and WCSPH methods to solve fluid-structure interaction problems

H. Sabahi and A.H. Nikseresht*

Department of Mechanical Engineering, Shiraz University of Technology, Shiraz, P.O. Box 71555-313, Iran.

Received 3 November 2014; received in revised form 21 December 2015; accepted 8 February 2016

KEYWORDS
Incompressible Smoothed Particle Hydrodynamics (ISPH);
Hypo-elastic gate;
Fluid-solid interaction.

Abstract. In this paper, the in-house code based on the smoothed particle hydrodynamics is proposed to simulate a Fluid-Solid Interaction (FSI) problem. This method is a Lagrangian, mesh-free method, and it has a high ability to capture the free surface in two-phase flows and also the interface in FSI problems. To compare Weakly Compressible SPH (WCSPH) and Incompressible SPH (ISPH) schemes, fluid flow under a hypo-elastic gate is simulated in solid and fluid domains with both methods. At first, fluid domain is simulated with ISPH method and solid domain is solved with WCSPH scheme. Another simulation is done with both fluid and solid parts solved by WCSPH method. The results of both methods are in good agreement with each other and also with other researcher's results. So, it is concluded that it is easier to model the fluid flow with ISPH scheme and the solid part with WCSPH in coupling fluid-solid interaction problems with good accuracy.

1. Introduction

The interaction of a moveable or deformable structure with an internal or external fluid flow is called Fluid-Solid Interaction (FSI). Hydrodynamic damping of offshore structures in wave, oscillation of aircraft wings, and the flow of blood through arteries are some well-known examples of such phenomena.

The arbitrary Lagrangian Eulerian [1] and the Coupled Eulerian Lagrangian (CEL) methods are the most popular methods to solve the FSI problems. In both methods, Eulerian and Lagrangian formulations are coupled to obtain the advantages of each pure method and prevent the disadvantages of each uncoupled formulations. In problems with small deformation, ALE methods have high accuracy and low computational cost, but in the problems of large deformation, these coupled methods need the re-meshing procedure and re-meshing has high computational cost. Smoothed Particle Hydrodynamics (SPH) is a mesh-free, Lagrangian and particle adaptive method which has a high ability to solve the large deformation fluid-solid interaction problems. This method has a good ability to track the free surface and find the interface in FSI problems. Easy implementation of SPH group methods for solving fluid flows around complex geometries is another advantage of these schemes.

There are two approaches in the SPH method to find the pressure of the particles; one is the use of Weakly Compressible SPH (WCSPH) idea, in which an equation of state is solved to find the pressure. Another approach is Incompressible SPH (ISPH) which is introduced by Cummins and Rudman [2], and in which incompressibility is enforced by solving Poisson equation. It seems that solving the Poisson equation in ISPH method decreases computational speed in each time step, but it should be noted that in WCSPH method, the speed of sound is used to satisfy the

*. *Corresponding author. Tel./Fax: +98 71 37264102;*
E-mail addresses: H.sabahi@sutech.ac.ir (H. Sabahi);
nikser@sutech.ac.ir (A.H. Nikseresht)

CFL condition and it leads to much smaller time steps in comparison with the ISPH method and more computational cost [3].

The SPH method was first introduced in astrophysics by Lucy [4] and also by Gingold and Monaghan [5]. Nowadays, this method is used to study different problems such as interfacial flows, that is, flow fields with different fluids separated by sharp interfaces [6], free surface and viscoelastic free surface flows [7-9], multi-fluid flows [10], wave interactions with porous media [11], and incompressible flows in general [12].

Recently, different algorithms of the SPH method are used to solve FSI problems. Antoci et al. [13] used a standard SPH method to model fluid-structure interaction problems. They neglected the effect of viscosity and used a repulsive force to prevent the penetration of fluid particles into the solid particles. Yang et al. [14] used a combined SPH-FEM model to simulate FSI problems. ISPH method is also utilized to solve some FSI problems by Rafiee and Thiagarajan [15]. They used Antoci's model for coupling conditions on the interface, and they also considered the viscosity of fluid.

The motivation of this work is to show the merits of the ISPH method. For this purpose, the in-house code is implemented based on SPH method. The fluid flow in a fluid-structure problem is solved by both ISPH and WCSPH methods. In both algorithms, the motion of the solid structure is modeled with WSCPH method. The results and methods of implementation in both algorithms are compared with each other.

2. Governing equations and numerical method

2.1. Governing equations

The equations of motion for two dimensional problems in the Lagrangian description include the conservation of mass and momentum which are as follows:

$$\frac{D\rho}{Dt} = -\rho \nabla . \vec{v}, \tag{1}$$

$$\frac{Dv_i}{Dt} = \frac{1}{\rho}\frac{\partial \sigma_{ij}}{\partial x_j} + f_i, \tag{2}$$

where t, ρ, v, f, and σ are time, density, velocity vector, external force, and stress tensor, respectively. The indices i and j refer to the ith and jth components of a vector. For fluids, the stress tensor can be decomposed into isotropic pressure, P, and shear stress, τ, as follows:

$$\sigma_{ij} = -P\delta_{ij} + \tau_{ij}. \tag{3}$$

The shear stress for Newtonian fluid is as follows:

$$\left(\frac{1}{\rho}\nabla . \tau\right)_i = \left(\frac{\mu}{\rho}\nabla^2 \vec{v}\right)_i, \tag{4}$$

where μ is the dynamic viscosity.

Eqs. (1) and (2) are also valid for solids. The stress tensor can be decomposed into isotropic pressure, P, and deviatoric shear stress tensor:

$$\sigma_{ij} = -P\delta_{ij} + S_{ij}, \tag{5}$$

where δ is the Kronecker delta. The deviatoric shear stress tensor can be obtained from Eq. (6) [16]:

$$\frac{DS_{ij}}{Dt} = 2\mu_s \left(D_{ij} - \frac{1}{3}D_{mm}\delta_{ij}\right) + S_{ik}W_{jk} + S_{kj}W_{ik}, \tag{6}$$

where μ_s, D, and W are the shear modulus, rate of deformation tensor, and spin tensor, respectively. D and W can be obtained from Eqs. (7) and (8):

$$D_{ij} = \frac{1}{2}\left(\frac{\partial v_i}{\partial x_j} + \frac{\partial v_j}{\partial x_i}\right), \tag{7}$$

$$W_{ij} = \frac{1}{2}\left(\frac{\partial v_i}{\partial x_j} - \frac{\partial v_j}{\partial x_i}\right). \tag{8}$$

2.2. Introduction to SPH

The SPH method is based on the integral interpolation theory. The value of any function in the SPH method is obtained by the values of the neighboring particles. Eq. (9) is the main idea in the SPH method [2]:

$$f(x) = \int f(x')\,\delta(x - x')\,dx', \tag{9}$$

where δ is the Kronecker delta. The continuous domain should be discretized, and the smoothing kernel function (w) is used instead of δ and the domain is represented by some particles, so the function $f(x)$ can be represented as:

$$\langle f(x)\rangle_a = \sum_{j=1}^{N} \frac{m_b}{\rho_b} f(x_b) w(x - x_b, h), \tag{10}$$

where m is the mass of particles, h is the smoothing length which defines the influence domain of the weight function, N is the number of neighboring particles, and indices a and b represent the central particle and its neighboring, respectively. The smoothing kernel function should have the following properties:

$$\begin{cases} \lim\limits_{x \to x'} w(x - x')dx' = \delta(x - x') \\ w(x - x') = 0 \qquad |x - x'| > kh \\ \int_\Omega w(x - x')dx' = 1 \end{cases} \tag{11}$$

In addition, the first and second derivatives should exist.

The stability of the SPH algorithm is dependent on the second derivative of the kernel function [17]. In

this paper, the cubic spline smoothing kernel function with the following formulation is used [15,18]:

$$w(r,h)=\begin{cases}\frac{10}{7\pi h^2}\left(1-\frac{3}{2}R^2+\frac{3}{4}R^3\right) & R<1\\ \frac{10}{28\pi h^2}(2-R)^3 & 1\le R\le 2\\ 0 & R>2\end{cases} \quad (12)$$

where $R=\frac{r}{h}$, r is the distance between particles, h is set to $h=1.3dx$, and dx is the initial horizontal distance between two neighboring particles. According to Eq. (12), particle b is a neighbor for particle a if $r_{ab}<2h$.

2.3. SPH approximation of divergence, gradient, and Laplasian operators

Divergence of the vector $\vec{V}$ and gradient of a function $f(x)$ can be obtained as follows [19]:

$$\frac{\nabla.\vec{V}}{\Delta t}=\frac{\sum_{b=1}^{N} m_b\left(\vec{V}_a-\vec{V}_b\right).\nabla_a W_{ab}}{\Delta t}, \quad (13)$$

$$\langle\nabla f(x_a)\rangle=\rho_a\sum_{b=1}^{N} m_b\left[\frac{f(x_b)}{\rho_b^2}+\frac{f(x_a)}{\rho_a^2}\right]\nabla_a w_{ab}, \quad (14)$$

in which:

$$\nabla_a w_{ab}=\left(\frac{\partial w}{\partial r_{ab}}\frac{x_a-x_b}{|r_{ab}|},\frac{\partial w}{\partial r_{ab}}\frac{y_a-y_b}{|r_{ab}|}\right). \quad (15)$$

The SPH approximation of Eq. (4) is:

$$\left(\frac{\mu}{\rho}\nabla^2\vec{v}\right)_a=\sum_b\frac{4m_b(\mu_a+\mu_b)\vec{r}_{ab}.\nabla_a w_{ab}}{(\rho_a+\rho_b)^2\left(|r_{ab}|^2+\eta^2\right)}\left(\vec{v}_a-\vec{v}_b\right), \quad (16)$$

where $\eta=0.1h$ is a non-zero parameter to prevent the denominator from getting zero.

2.4. SPH approximation of continuity and momentum equations

According to Eq. (10), the density can be found as follows:

$$\rho_a=\sum_{b=1}^{N}\rho_b w\frac{m_b}{\rho_b}=\sum_{b=1}^{N} w m_b. \quad (17)$$

Another form of density variation which is found from continuity equation can be written as in Eq. (18):

$$\frac{d\rho_a}{dt}=\rho_a\sum_{b=1}^{N}\frac{m_b}{\rho_b}(u_a-u_b).\nabla_a w_{ab}. \quad (18)$$

According to Eqs. (16) and (14), the SPH approximation of the momentum Eq. (2) for fluid can be obtained as:

$$\frac{Dv_{ai}}{Dt}=-\sum\nolimits_b m_b\left(\frac{P_a}{\rho_a^2}+\frac{P_b}{\rho_b^2}\right)\frac{\partial w_{ab}}{\partial_a x_i}+\sum_b\frac{4m_b(\mu_a+\mu_b)\vec{r}_{ab}.\nabla_a w_{ab}}{(\rho_a+\rho_b)^2\left(|r_{ab}|^2+\eta^2\right)}\left(\vec{v}_{ai}-\vec{v}_{bi}\right)+f_i. \quad (19)$$

Generally, in the SPH method, there are two schemes to find the pressure. The pressure in the standard form of the SPH is obtained from an equation of state; this form is called Weakly Compressible SPH (WCSPH). The equation of state for both parts (fluid and solid) has the form of Eq. (20):

$$P=c_0^2(\rho-\rho_0). \quad (20)$$

In the solid, $c_0^2=\frac{k}{\rho_0}$ where k is the bulk modulus and for the fluid, $c_0^2=\frac{\zeta}{\rho_0}$ where ζ is the compressibility modulus where ρ_0 is the reference density. The WCSPH method cannot satisfy incompressibility, there is another form of SPH to satisfy incompressibility, and this form is called Incompressible SPH (ISPH). In the ISPH method, pressure is obtained from the Poisson equation, and the continuity equation is satisfied by vanishing velocity divergence. The Poisson equation can be found as [2]:

$$\nabla.\left(\frac{1}{\rho}\nabla P_{t+1}\right)=\frac{\nabla.\vec{v}}{\Delta t}. \quad (21)$$

The left-hand side of Eq. (21) is discretized as follows [10,20]:

$$\nabla.\left(\frac{1}{\rho}\nabla P\right)_a=\sum_b^N m_b\frac{8}{(\rho_a+\rho_b)^2}\frac{(P_a-P_b)\vec{r}_{ab}.\nabla_a w_{ab}}{|r_{ab}|^2+\eta^2}, \quad (22)$$

where $\vec{r}_{ab}=\vec{r}_a-\vec{r}_b$. The momentum equation for solid particles can be written as:

$$\frac{Dv_{ai}}{Dt}=-\sum_b m_b\left(\frac{P_a}{\rho_a^2}+\frac{P_b}{\rho_b^2}+\prod_{ab}\right)\frac{\partial w_{ab}}{\partial_a x_i}+\sum_b m_b\left(\frac{S_{ija}}{\rho_a^2}+\frac{S_{ijb}}{\rho_b^2}+(R_{ija}+R_{ijb})f^n\right)\frac{\partial w_{ab}}{\partial_a x_j}+f_i, \quad (23)$$

where $\prod_{ab}$ is an artificial viscosity and R_{ij} is an artificial stress, these two terms have been introduced in order to solve numerical problems. $\prod_{ab}$ has been proposed by [21] and can smooth out the velocity oscillations when particles get too close to each other:

$$\prod_{ab}=\begin{cases}\frac{-\alpha\bar{c}_{ab}\mu_{ab}}{\bar{\rho}_{ab}} & \vec{v}_{ab}.\vec{r}_{ab}<0\\ 0 & \vec{v}_{ab}.\vec{r}_{ab}>0\end{cases} \quad (24)$$

where:

$$\vec{r}_{ab} = \vec{r}_a - \vec{r}_b,$$

$$\vec{v}_{ab} = \vec{v}_a - \vec{v}_b,$$

$$\mu_{ab} = \frac{h\left(\vec{v}_{ab}.\vec{r}_{ab}\right)}{\left|r_{ab}\right|^2 + 0.01h^2},$$

$$\bar{\rho}_{ab} = \frac{1}{2}(\rho_a + \rho_b), \quad \text{and} \quad \bar{c}_{ab} = \frac{1}{2}(c_a + c_b).$$

c is the speed of sound and α is an artificial viscosity coefficient. According to the following equations, the component of R_{ij} can be obtained:

$$\bar{R}_a^{xx} = \begin{cases} -e\frac{\bar{\sigma}_a^{xx}}{\rho_a^2} & \bar{\sigma}_a^{xx} > 0 \\ 0 & \bar{\sigma}_a^{xx} < 0 \end{cases} \tag{25}$$

$$\bar{R}_a^{yy} = \begin{cases} -e\frac{\bar{\sigma}_a^{yy}}{\rho_a^2} & \bar{\sigma}_a^{yy} > 0 \\ 0 & \bar{\sigma}_a^{yy} < 0 \end{cases} \tag{26}$$

To obtain R_{ij}, it is necessary to find principal stresses [16]:

$$\bar{\sigma}_a^{xx} = c^2\sigma_a^{xx} + 2sc\sigma_a^{xy} + s^2\sigma_a^{yy}, \tag{27}$$

$$\bar{\sigma}_a^{yy} = s^2\sigma_a^{xx} + 2sc\sigma_a^{xy} + c^2\sigma_a^{yy}, \tag{28}$$

where c and s represent $\cos\theta$ and $\sin\theta$, and:

$$\tan 2\theta_a = \frac{2\sigma_a^{xy}}{\sigma_a^{xx} - \sigma_a^{yy}}, \tag{29}$$

$$\bar{R}_a^{xx} = \begin{cases} -e\frac{\bar{\sigma}_a^{xx}}{\rho_a^2} & \bar{\sigma}_a^{xx} > 0 \\ 0 & \bar{\sigma}_a^{xx} < 0 \end{cases} \tag{30}$$

$$\bar{R}_a^{yy} = \begin{cases} -e\frac{\bar{\sigma}_a^{yy}}{\rho_a^2} & \bar{\sigma}_a^{yy} > 0 \\ 0 & \bar{\sigma}_a^{yy} < 0 \end{cases} \tag{31}$$

e is a constant and is set to $e = 0.3$.

$$R_a^{xx} = c^2\bar{R}_a^{xx} + s^2\bar{R}_a^{yy}, \tag{32}$$

$$R_a^{yy} = s^2\bar{R}_a^{xx} + c^2\bar{R}_a^{yy}, \tag{33}$$

$$R_a^{xy} = cs\left(\bar{R}_a^{xx} - \bar{R}_a^{yy}\right). \tag{34}$$

$f = \frac{w_{ij}}{w(l_0,h)}$ where l_0 is the initial distance between two neighboring particles, and n is set to 4.

Eqs. (7) and (8) are discretized in order to found deviatoric stress tensor.

$$D_{xx} = -\sum_b \frac{m_b}{\rho_b}(u_a - u_b)\frac{\partial w}{\partial x}, \tag{35}$$

$$D_{yy} = -\sum_b \frac{m_b}{\rho_b}(v_a - v_b)\frac{\partial w}{\partial y}, \tag{36}$$

$$D_{xy} = D_{yx} = -\frac{1}{2}\sum_b \frac{m_b}{\rho_b}\left[(u_a - u_b)\frac{\partial w}{\partial y} + (v_a - v_b)\frac{\partial w}{\partial x}\right], \tag{37}$$

$$W_{xy} = -\frac{1}{2}\sum_b \frac{m_b}{\rho_b}\left[(u_a - u_b)\frac{\partial w}{\partial y} - (v_a - v_b)\frac{\partial w}{\partial x}\right], \tag{38}$$

$$W_{xx} = W_{yy} = 0. \tag{39}$$

Finally, the components of deviatoric stress tensor can be found as:

$$\frac{S_{ij}^{n+1} - S_{ij}^n}{\Delta t} = 2\mu_s\left(D_{ij}^n - \frac{1}{3}D_{mm}^n\delta_{ij}\right) + S_{ik}^{n+1}W_{jk}^n + S_{kj}^{n+1}W_{ik}^n. \tag{40}$$

2.5. Free surface and wall boundary condition

The base rule of finding free surface interface in the SPH methods is the variation of density near the free surface. Due to the fact that the surface particles in free surface have less neighboring particles, the density of these particles decreases according to Eq. (17), as depicted in Figure 1. Therefore, a particle is considered in the free surface if $\rho < \beta\rho_0$ where $0.8 < \beta < 0.99$ [22].

In this research, dummy particles are used to prevent the penetration of fluid particles into the solid particles in the wall boundary conditions. This method was purposed by Koshizuka et al. [23]. Two sets of particles are used in this method; the first set of particles are placed on the boundary as shown in Figure 2, and the second set of particles are used

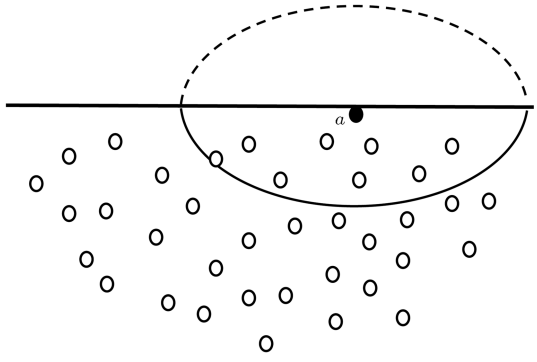

Figure 1. Position of free surface particles.

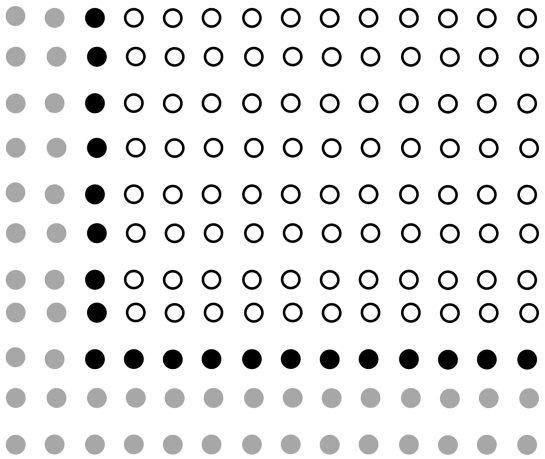

Figure 2. Three rows of dummy particles in the boundary.

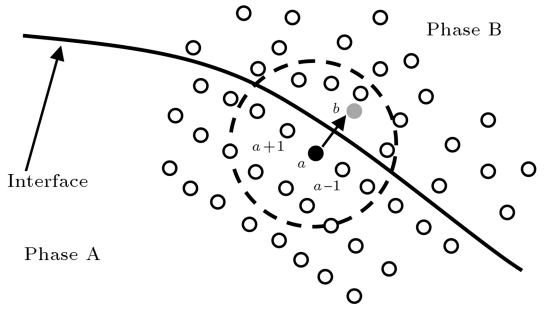

Figure 3. Interface and its normal vector.

to avoid density change close to the boundary. The Poisson equation is solved to calculate the pressure of dummy particles and the velocity is set to zero.

2.6. Fluid-solid interaction model

In the SPH method, each particle has a support domain. All particles with the distance of $2h$ or lower than $2h$ are in the support domain of the central particle. In FSI problems, there are two sets of particles (fluid and solid) close to the interface. Thus, the support domain of the interface particles included both solid and fluid particles (like particles a and b in Figure 3). By extending the summation of Eqs. (19) and (23) to all particles regardless of their nature, the coupling condition can be satisfied [13].

In the previous works, some repulsive forces were used to prevent the penetration of fluid particles into the solid particles [13,14,24]. The previously used repulsive forces are complex and are sometimes dependent on the fluid particles pressure. In the present work, a new repulsive force is introduced that is very easy to implement and it is not dependent on pressure. This repulsive force was first proposed by Esmaeili [25] for wall boundary condition. This force works as an external force and exert from solid particles to the fluid particles. Also, the dynamic interface condition is satisfied by exerting the repulsive force on the opposite direction to solid particles [14]. This new repulsive force which is used in the present FSI problem with WCSPH method can be depicted as follows:

$$f = \begin{cases} \frac{1}{3}\left(\frac{-\overrightarrow{u^{t-1}}.\vec{n}}{dt}\right)\left(\frac{1-0.5q}{0.5q}\right) & \vec{u}.\vec{n} < 0 \\ 0 & \vec{u}.\vec{n} > 0 \end{cases} \tag{41}$$

where $q = \frac{|r_{ij}|}{2h}$ $(0 < q < 1)$ and $\vec{n}$ is the normal to the interface particles. The tangential vector of solid particles which are near to the interface can be found as in [26]:

$$\widehat{t}_a = (t_{ax}, t_{ay}) = \left(\frac{x_{a+1} - x_{a-1}}{|r_{a+1,a-1}|}, \frac{y_{a+1} - y_{a-1}}{|r_{a+1,a-1}|}\right), \tag{42}$$

where $a-1$ and $a+1$ represent the two particles which are before and after the particle a, respectively, as is shown in Figure 3. The vertical vector at particle a can be found as:

$$\vec{n}_a = (-t_{ay}, t_{ax}). \tag{43}$$

In a few papers, the ISPH method was used to simulate FSI problems [15]. In this method, incompressibility is satisfied by the Poisson equation. In this paper, to compare the implementation of WCSPH and ISPH methods, fluid particles of a FSI problem are simulated by both WSCPH and ISPH methods. In the ISPH method, there is no need to use the repulsive force, and it is one of the merits of the ISPH method.

In both WCSPH and ISPH methods, to model the fluid-solid interaction problems, in each time step, at first, the fluid domain is solved and the fluid particles are moved with their calculated velocities. Afterwards, the exerted force by the fluid particles on the solid particles are obtained, so the solid domain equation is solved and the solid particles are moved to their new locations. In the WCSPH method, to prevent the penetration of fluid particles into the solid domain, a repulsive force is implemented. So, in each time step, the repulsive force is specified and exerted on the fluid particles from solid particles; it is also exerted from the fluid particles on the solid particles according to the Newtown's third law.

2.7. XSPH velocity correction

In order to smooth out oscillation of particles velocity, the XSPH technique is used. In this technique, particles move with a velocity closer to the average velocity, and particles are moved by [27]:

$$\frac{D\vec{r}_a}{Dt} = \overrightarrow{v_a} - \varepsilon \sum_b \frac{m_b}{\overline{\rho_{ab}}} \left(\overrightarrow{v_a} - \overrightarrow{v_b}\right) w_{ab}, \tag{44}$$

where $\overline{\rho_{ab}} = \frac{\rho_a + \rho_b}{2}$, and ε is set to 0.5.

2.8. ISPH algorithm

In the ISPH algorithm, a prediction-correction scheme is used for time marching. So, the complete movement of the fluid particles is achieved after finishing the two sub steps of each time step. In the prediction step, particles move without sensing the effect of pressure gradient and the temporal particle position, and velocity can be founded by solving the momentum equation only by considering the body and shear forces with the following equations [2]:

$$\vec{r}_* = \vec{r}_t + \vec{v}_t \Delta t, \tag{45}$$

$$\Delta \vec{v}_* = \left(\vec{g} + \frac{\mu}{\rho} \nabla^2 \vec{v} \right) \Delta t, \tag{46}$$

$$\vec{v}_* = \vec{v}_t + \Delta \vec{v}_*, \tag{47}$$

where subscripts t and $*$ denote the parameters at time t and in the prediction step. After finding the position and velocity in the prediction step, the density in this step can be obtained from Eq. (17). In the second sub step (correction step), the effect of pressure gradient is considered. The pressure in this new time step $(t+1)$ can be found by solving the Poisson equation [28]:

$$\nabla . \left(\frac{1}{\rho_*} \nabla P_{t+1} \right) = \frac{\nabla . \vec{v}_*}{\Delta t}. \tag{48}$$

In the correction step, incompressibility is satisfied, and the position and velocity are corrected as follows:

$$\vec{v}_{t+1} = \vec{v}_* + \Delta \vec{v}_{**}, \tag{49}$$

$$\vec{r}_{t+1} = \vec{r}_t + \frac{\vec{v}_t + \vec{v}_{t+1}}{2} \Delta t, \tag{50}$$

where subscript $**$ represents the correction step and $\overrightarrow{\Delta v_{**}}$ is:

$$\Delta \vec{v}_{**} = -\frac{1}{\rho_*} \nabla P_{t+1} \Delta t. \tag{51}$$

3. Results and discussion

3.1. Fluid flow under a gate

To validate the fluid part of the prepared code, a fluid flow under a gate is solved by the ISPH method, and results are compared with the finite volume and VOF scheme. The fluid is water with $\rho = 1000 \ \frac{\text{kg}}{\text{m}^3}$, $\mu = 0.001 \ \frac{\text{N}}{\text{m}^2\text{s}}$, and $g = 9.81 \ \frac{\text{m}}{\text{s}^2}$. The geometry is a tank with the length and the height of 0.1 and 0.14 m, respectively. Also the height of the gate is 0.03 m. In this simulation, the total number of particles is 1689; the initial space between the particles is 0.00375 m, and the time step is set to 0.001 s. To check the independency from the number of particles, this example is also simulated with 2580 particles. The size of the particles adjacent to the gate is set to 0.001 m. After that, the particles size is set to 0.002 m and adjusted to 0.00375 m far from the gate. The comparison of fluid flow under the gate with ISPH and VOF schemes is depicted in Figure 4 for different particle sizes and shows similar results with a reasonable agreement. It also shows the ability of the ISPH method to capture the free surface flows [28]. This example is also solved by WCSPH method with 1689 particles.

Figure 5 shows the pressure distribution of fluid flow under the gate for two different time steps.

3.2. Oscillating plate

For validating the solid part of the code, vibration of an elastic plate is simulated [13,16]. The plate has one end clamped and the other end is free, as is shown in Figure 6. In this example, the plate is initially horizontal and oscillates around the initial position of its fundamental mode ($kL = 1.875$). According to the analytical expression of the first normal mode, the initial velocity distribution is:

$$v_y = c_0 v_{0L} \frac{f(x)}{f(L)}, \tag{52}$$

where:

$$f(x) = (\cos(kL) + \cosh(kL))(\cosh(kx) - \cos(kx)) + (\sin(kL) - \sinh(kL))(\sinh(kx) - \sin(kx)), \tag{53}$$

and $v_{0L} = 0.01$ is the initial velocity of the free end of the plate, and other properties are: $L = 0.2$ m, $H = 0.02$ m, $\rho = 1000 \ \frac{\text{kg}}{\text{m}^3}$, $\mu_s = 7.15 \times 10^6 \ \frac{\text{N}}{\text{m}^2}$, and $K = 3.25 \times 10^6 \ \frac{\text{N}}{\text{m}^2}$. The results are compared with the analytical solution and also with the other researchers' results (Table 1).

This example is solved by WCSPH method along with two sets of particles, $n = 3195$ and $n = 5560$ particles; the time step is set to $\Delta t = 10^{-5}$ second. The results are in good agreement with other results as depicted in Figure 7.

3.3. Fluid flow under a hypo-elastic gate

In this part, the deformation of an elastic gate due to water pressure is simulated to show the ability of ISPH method in FSI problems. The elastic gate is clamped

Table 1. Non-dimensional parameters.

	Non-dimensional period $\left(\frac{T c_0}{L}\right)$	Non-dimensional amplitude $\left(\frac{A}{L}\right)$
Present SPH	80.95	0.125
Antoci et al. [13]	81.5	0.124
Gray et al. [16]	82	0.125
Analytical solution	72.39	0.115

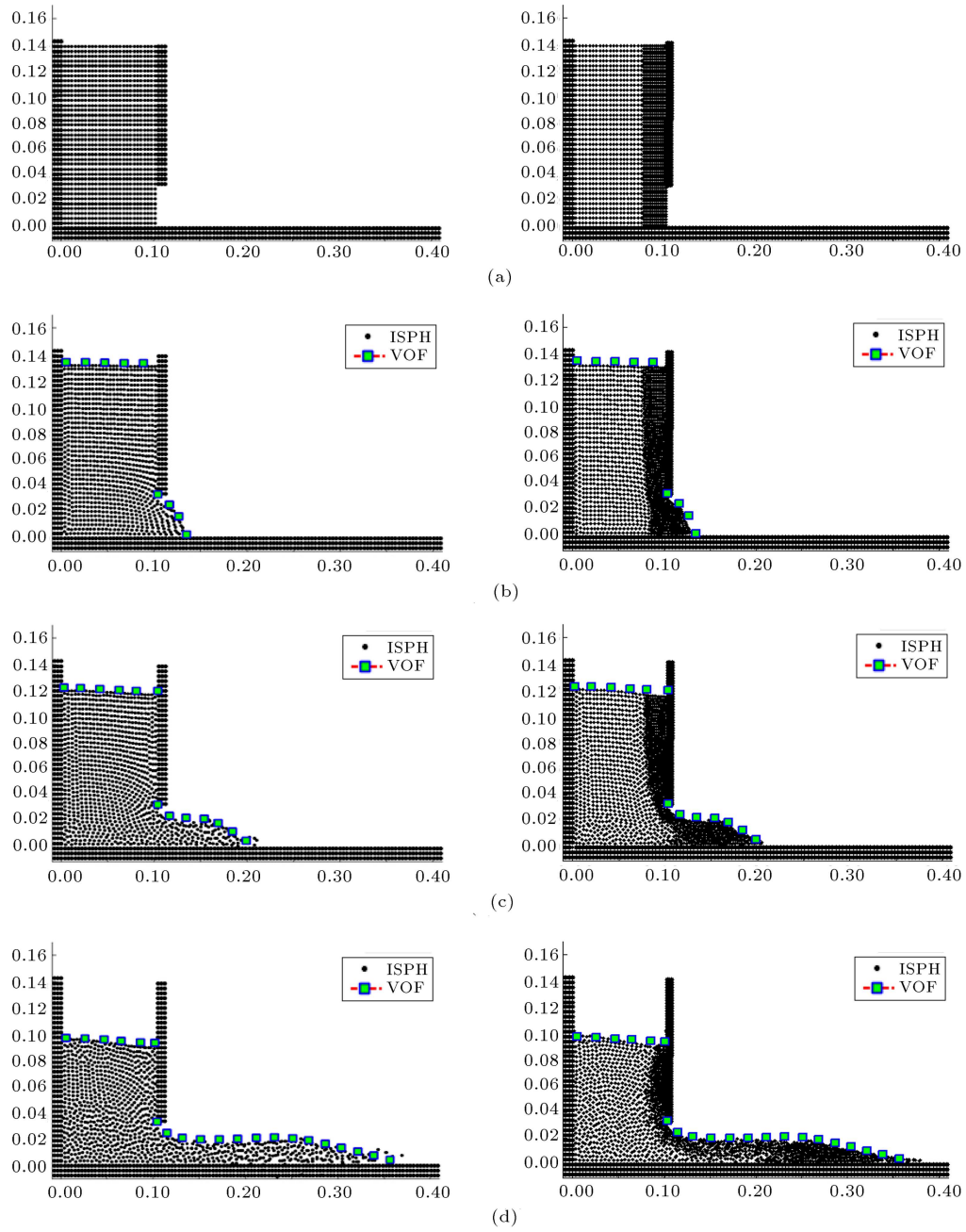

Figure 4. The comparison of fluid flow under the gate with ISPH and VOF methods at times (a) 0.0 s, (b) 0.05 s, (c) 0.1 s, and (d) 0.2 s (left: 1689 particles and right: 2580 particles).

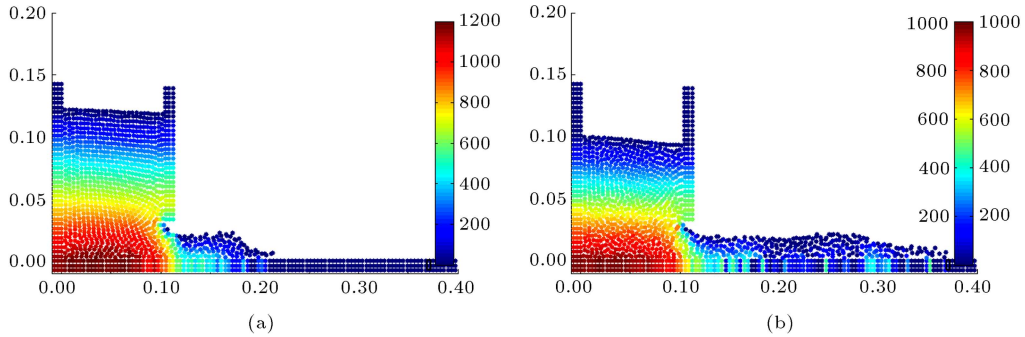

Figure 5. The pressure distribution of fluid flow under the gate with ISPH: (a) 0.1 s; and (b) 0.2 s.

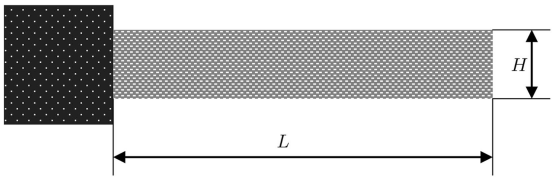

Figure 6. Geometry of the plate.

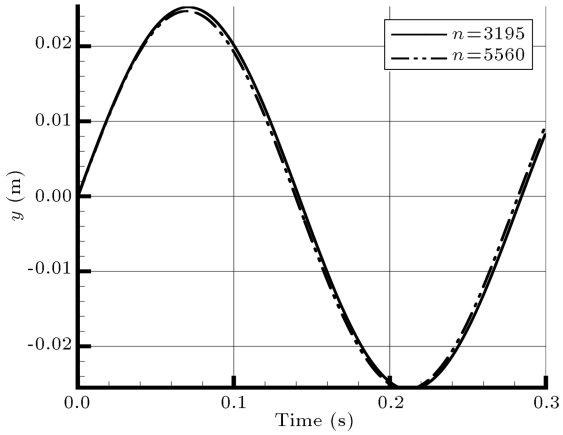

Figure 7. Vertical displacement of the free end of the plate by $n = 3195$ and $n = 5560$ particles.

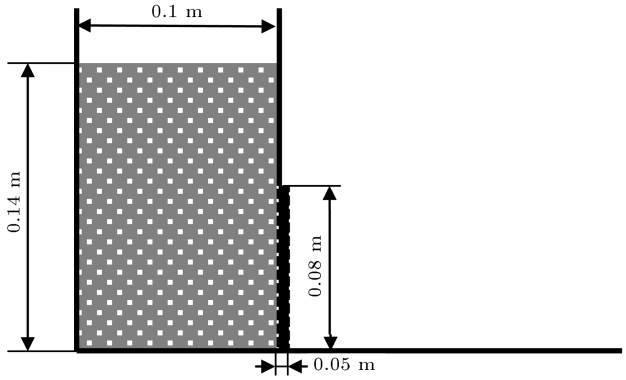

Figure 8. Initial configuration and geometry of hypoelastic gate.

at one end and free at the other end. The geometry of this example is shown in Figure 8.

In this example, ISPH method is used to find the pressure of fluid particles, and WCSPH method is used to calculate the pressure of solid particles.

The fluid properties are $\rho = 1000\ \frac{\text{kg}}{\text{m}^3}$ and $\mu = 0.001\ \frac{\text{N}}{\text{m}^2\text{s}}$. The elastic plate properties are $K = 2 \times 10^7\ \frac{\text{N}}{\text{m}^2}$, $\mu_S = 4.27 \times 10^6\ \frac{\text{N}}{\text{m}^2}$, and $\rho = 1100\ \frac{\text{kg}}{\text{m}^3}$. The accuracy of the SPH method can be improved by increasing the number of particles, but the computational cost increases by increasing the total number of particles. So, in the present work, smaller particles are used close to the places of high gradient, and bigger particles are used in other parts of the domain. For particles a and b with different sizes, the smoothing length is set to $h = \sqrt{h_a h_b}$. In this example, there are 6672 particles in total. The initial spacing between solid particles is set to 0.001 m, for fluid particles close to the gate is set to 0.001 m, and far from the gate is set to 0.002 m. To insure numerical stability, the time step is set to $\Delta t = 3 \times 10^{-6}$ second. Figure 9 shows the comparison of the present results with the results of Antoci et al. [13] with the increment of 0.04 second. The particle clustering near the free surface flow is not seen in this research. It is due to the use of the XSPH scheme which is a method to prevent the particle clustering. The results are in good agreement with each other. This example was also simulated with 4945 particles and the results show no significant changes. To compare the implementation of WCSPH and ISPH methods, the example is again solved by WCSPH method (in both media, fluid and solid) with two sets of particles (6667 and 9069). As mentioned earlier, in the present ISPH method, the repulsive force is not used and this is an advantage of this work; another merit is also the coupling of ISPH and WCSPH methods.

Figure 10 shows the pressure distribution under a hypo-elastic gate for four different time steps.

Figures 11 and 12 show the comparison of the present horizontal and vertical displacement components of the free end of the plate with the experimental results of Antoci et al. [13] and numerical results of Rafiee et al. [15].

Figures 11 and 12 depict that both ISPH and WCSPH methods have reasonable accuracy, but the ISPH method, especially in vertical displacement, shows higher accuracy. The higher accuracy of ISPH method is due to solving Poisson equation for finding the pressure distribution; therefore, it does not need to use a repulsive force. Furthermore, the number of particles used in the ISPH method is less than the number of particles used in the WCSPH method (4945 particles versus 6667 particles).

Figures 11 and 12 show that ISPH method of Rafiee's work has also higher accuracy with respect to WCSPH method. Rafiee et al. [15] used the complex integral method algorithm of Antoci et al. [13] in coupling the FSI problem, and they also used a highly pressure-dependent formulation in their repulsive force. But, in the present work, a simple coupling of FSI problem without using any repulsive force in ISPH method is used, and the results show good agreement with the experiments, especially in the vertical displacement. On the other hand, Rafiee et al. simulated the problem with 6928 particles, but only 4945 particles are used in the present work.

4. Conclusion

In the present work, both the WCSPH and ISPH methods are used to solve the fluid part, and the

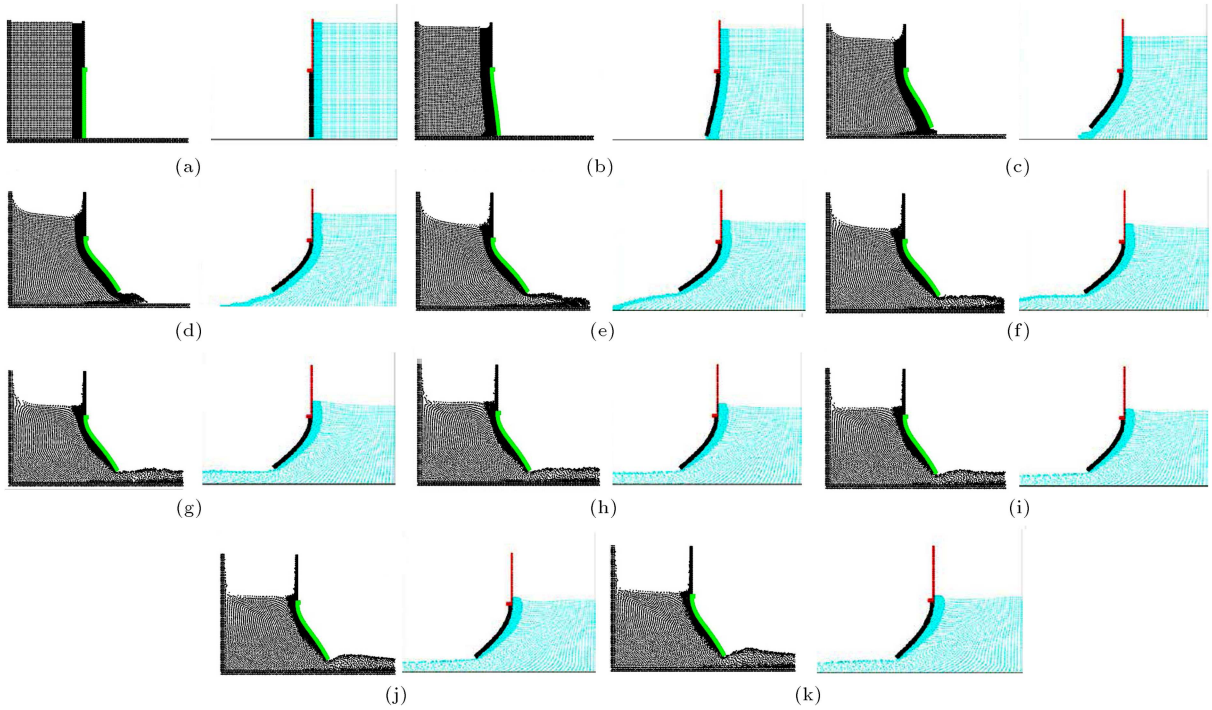

Figure 9. Comparison of the present study with the results of Antoci et al. [13] with increment of 0.04 second from $t = 0$ s.

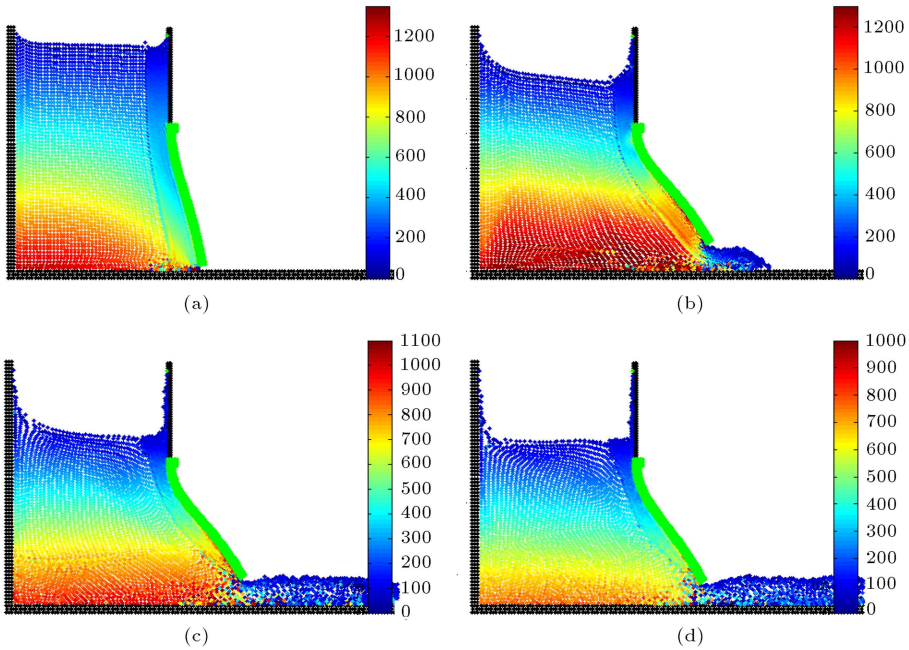

Figure 10. The pressure distribution of fluid flow under a hypo-elastic gate: (a) 0.054 s; (b) 0.117 s; (c) 0.207 s; and (d) 0.288 s.

WCSPH method is used to solve the solid part of a FSI problem. In the WCSPH method, an easy repulsive force which is not pressure-dependent is introduced. In the ISPH method, the pressure of fluid particles is obtained by solving the Poisson equation, and the incompressibility is satisfied, also the fluid and solid parts are coupled without using any repulsive force. Results of the present coupling of the ISPH and WCSPH are in good agreement with other experimental and numerical data. It is shown that the ISPH coupling with WCSPH has higher accuracy with respect to the use of WCSPH method in both fluid and solid parts of a FSI problem. Therefore, it is concluded that this coupling without using any repulsive force is very easy to implement and has enough accuracy and robustness to solve the FSI problems.

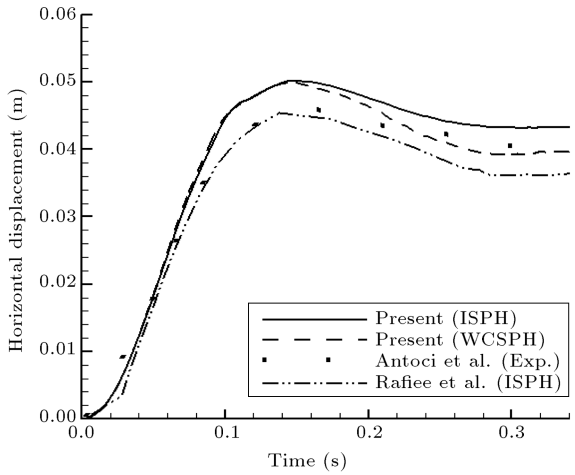

Figure 11. The horizontal displacement component of the free end of the plate.

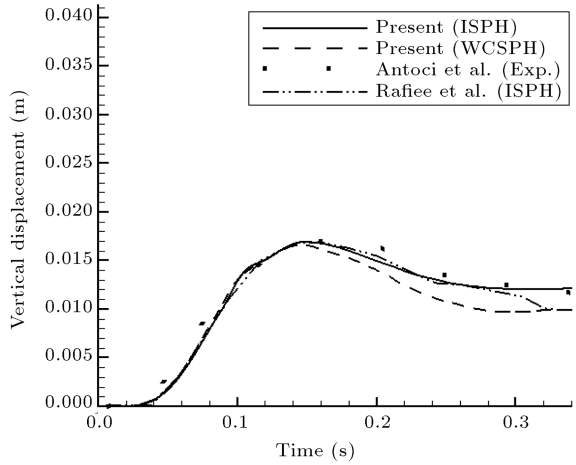

Figure 12. The vertical displacement component of the free end of the plate.

References

1. Rugonyi, S. and Bathe, K. "On finite element analysis of fluid flows fully coupled with structural interactions", *CMES- Computer Modeling in Engineering and Sciences*, **2**(2), pp. 195-212 (2001).
2. Cummins, S.J. and Rudman, M. "An SPH projection method", *Journal of Computational Physics*, **152**(2), pp. 584-607 (1999).
3. Sun, F. "Investigations of smoothed particle hydrodynamics method for fluid-rigid body interactions", PhD Thesis, University of Southampton (2013).
4. Lucy, L. "A numerical approach to the testing of fusion processes", *The Astronomical J.*, **82**, pp. 1013-1024 (1977).
5. Gingold, R.A. and Monaghan, J.J. "Smoothed particle hydrodynamics-theory and application to non-spherical stars", *Monthly Notices of the Royal Astronomical Society*, **181**, pp. 375-389 (1977).
6. Colagrossi, A. and Landrini, M. "Numerical simulation of interfacial flows by smoothed particle hydrodynamics", *J. Comput. Phys.*, **191**, pp. 448-475 (2003).
7. Rafiee, A., Manzari, M.T. and Hosseini, M. " An incompressible SPH method for simulation of unsteady viscoelastic free-surface flows", *Int. J. Non-Linear Mech.*, **42**, pp. 1210-1223 (2007).
8. Shao, S. "Incompressible smoothed particle hydrodynamics simulation of multifluid flows", *International Journal for Numerical Methods in Fluids*, **69**(11), pp. 1715-1735 (2012).
9. Antuono, M., Colagrossi, A., Marrone, S. and Molteni, D. "Free-surface flows solved by means of SPH schemes with numerical diffusive 361 terms", *Computer Physics Communications*, **181**, pp. 532-549 (2010).
10. Ghadampour, Z., Talebbeydokhti, N., Hashemi, M.R., Nikseresht, A.H. and Neill, S.P. "Numerical simulation of free surface mudflow using incompressible SPH", *IJST, Transactions of Civil Engineering*, **37**, pp. 77-95 (2013).
11. Shao, S. "Incompressible SPH flow model for wave interactions with porous media", *Coastal Engineering*, **57**, pp. 304-316 (2010).
12. Liu, G.R. and Liu, M.B., *Smoothed Particle Hydrodynamics: A Meshfree Particle Method*, World Scientific Publishing Co. Pte. Ltd. (2003).
13. Antoci, C., Gallati, M. and Sibilla, S. "Numerical simulation of fluid-structure interaction by SPH", *Computers & Structures*, **85**(11), pp. 879-890 (2007).
14. Yang, Q., Jones, V. and McCue, L. "Free-surface flow interactions with deformable structures using an SPH-FEM model", *Ocean Engineering*, **55**, pp. 136-147 (2012).
15. Rafiee, A. and Thiagarajan, K.P. "An SPH projection method for simulating fluid-hypo elastic structure interaction", *Comput. Methods Appl. Mech. Engrg.*, **198**, pp. 2785-2795 (2009).
16. Gray, J., Monaghan, J. and Swift, R. "SPH elastic dynamics", *Computer Methods in Applied Mechanics and Engineering*, **190**(49), pp. 6641-6662 (2001).
17. Morris, J.P., Fox, P.J. and Zhu, Y. "Modeling low Reynolds number incompressible flows using SPH", *J. Comp. Phys.*, **136**, pp. 214-226 (1997).
18. Monaghan, J. "Smoothed particle hydrodynamics", *Annu. Rev. Astron. Astrophys.*, **30**, pp. 543-574 (1992).
19. Liu, M.L.G. "Smoothed particle hydrodynamics (SPH): An overview and recent developments", *Archives of Computational Methods in Engineering*, **17**, pp. 25-76 (2010).
20. Shao, S. and Lo, E.Y. "Incompressible SPH method for simulating Newtonian and non-Newtonian flows with a free surface", *Advances in Water Resources*, **26**(7), pp. 787-800 (2003).
21. Monaghan, J. and Gingold, R. "Shock simulation by the particle method SPH", *Journal of Computational Physics*, **52**(2), pp. 374-389 (1983).

22. Koshizuka, S. and Oka, Y. "Moving-particle semi-implicit method for fragmentation of incompressible fluid", *J. Nucl. Sci. Engrg*, **123**, pp. 421-434 (1996).
23. Koshizuka, S., Nobe, A. and Oka, Y. "Numerical analysis of breaking waves using the moving particle semi-implicit method", *International Journal for Numerical Methods in Fluids*, **26**(7), pp. 751-769 (1998).
24. Schörgenhumer, M., Johannes, A. and Gerstmayr, J. "Smoothed particle hydrodynamics and model-order reduction for efficient modeling of fluid-structure interaction", *8th Vienna International Conference on Mathematical Modelling* - MATHMOD (2015).
25. Esmaili Sikarodi, M.A. "Using GPU in ISPH simulation of incompressible flows", Master of Science Thesis, Departeman of Mechanical and Aerospace Engineering, Shiraz University of Technology (2013) (in Persian).
26. Randles, P. and Libersky, L. "Smoothed particle hydrodynamics: some recent improvements and applications", *Computer Methods in Applied Mechanics and Engineering*, **139**(1), pp. 375-408 (1996).
27. Monaghan, J. "On the problem of penetration in particle methods", *J. Comput. Phys.*, **82**, pp. 1-15 (1989).
28. Ghadampour, Z., Hashemi, M.R., Talebbeydokhti, N., Neill, S.P. and Nikseresht, A.H. "Some numerical aspects of modelling flow around hydraulic structures using incompressible SPH ", *Computers and Mathematics with Applications*, **69**, pp. 1470-1483 (2015).

Biographies

Hooshang Sabahi received his BSc degree in Mechanical Engineering in 2010 from the Islamic Azad University, Shiraz Branch, Iran, and his MSc degree in Mechanical Engineering in 2014 from Shiraz University of Technology, Iran. Now, he is a PhD student of Shiraz University of Technology, Iran. His current research is focused on the SPH method.

Amir Hossein Nikseresht received his BSc, MSc, and PhD degrees from Shiraz University, Shiraz, Iran in 1995, 1997, and 2004, respectively, all in Mechanical Engineering. He is currently an Associate Professor of Mechanical Engineering in Shiraz University of Technology, Iran. His research interests include free surface flows, CFD, hydrodynamics, and mesh-less methods.